



ACADEMIC
PRESS

Available online at www.sciencedirect.com

SCIENCE @ DIRECT®

Archives of Biochemistry and Biophysics 411 (2003) 223–234

ABB

www.elsevier.com/locate/yabbi

Identification and regulation of a new vertebrate cytochrome P450 subfamily, the CYP2Ps, and functional characterization of CYP2P3, a conserved arachidonic acid epoxygenase/19-hydroxylase[☆]

Marjorie F. Oleksiak,^a Shu Wu,^b Carol Parker,^b Wei Qu,^b Rachel Cox,^a
Darryl C. Zeldin,^b and John J. Stegeman^{a,*}

^a *Biology Department, Woods Hole Oceanographic Institution, Woods Hole, MA 02543, USA*

^b *Laboratory of Pulmonary Pathobiology, National Institute of Environmental Health Sciences, Research Triangle Park, NC 27709, USA*

Received 20 August 2002, and in revised form 25 November 2002

Abstract

Three genes cloned from *Fundulus heteroclitus* (killifish) define a new P450 subfamily, CYP2P. Structurally, the CYP2Ps are related to fish CYP2Ns and mammalian CYP2Js. CYP2P transcripts are expressed predominantly in liver and intestine. CYP2P3 coexpressed with P450 oxidoreductase in a baculovirus system catalyzed benzphetamine-*N*-demethylation and arachidonic acid oxidation, forming 14,15-, 11,12-, and 8,9-epoxyeicosatrienoic acids and 19-hydroxyeicosatetraenoic acid. CYP2P3 regio- and enantioselectivities with arachidonic acid were remarkably similar to human CYP2J2 and rat CYP2J3. Epoxyeicosatrienoic acids and their corresponding hydration products, the dihydroxyeicosatrienoic acids, were detected in killifish liver and intestine, indicating metabolism of arachidonic acid by killifish P450s in vivo. Levels of these products in killifish intestine were higher than those in mammalian intestine. 12-*O*-Tetradecanoyl phorbol 13-acetate suppressed expression of CYP2P2 and CYP2P3 in killifish intestine; fasting itself suppressed expression of CYP2P2/3 but not CYP2P1. In rat intestine fasting similarly depressed the levels of CYP2J proteins. The CYP2Ps and the CYP2Js appear to be derived from a common ancestral gene, likely a fatty acid mono-oxygenase.

© 2003 Elsevier Science (USA). All rights reserved.

Eicosanoids derived from the metabolism of arachidonic acid (AA)¹ play critical roles in regulating numerous biological processes, such as salt and water transport [1], reproduction [2,3], and cellular proliferation [4] in animals. In mammals, different pathways of

AA metabolism are catalyzed by cyclooxygenases, lipoxygenases, and members of the superfamily of cytochrome P450 monooxygenases [5]. Cytochrome P450 proteins can oxygenate AA via olefin epoxidation, ω-terminal oxidation, and oxidation of allylic or bis-allylic carbons [6], forming four regioisomeric epoxyeicosatrienoic acids (EETs), which can be hydrated to the *vic*-dihydroxyeicosatrienoic acids (DHETs), and numerous hydroxyeicosatetraenoic acids (HETEs). Biological effects of EETs and HETEs in mammals include regulation of intracellular calcium concentrations, vasoactive effects, release of peptide hormones, and antiaggregatory effects on platelets [7,8]. AA metabolites formed by some mammalian P450s may have distinct roles; yet, the full physiological significance of P450 metabolism of AA remains enigmatic.

Many mammalian P450s in the CYP2 gene family are AA epoxygenases, while ω-terminal hydroxylation of

[☆] This research was supported in part by a multi-investigator Sea Grant Research Enhancement Program, NA46RG0470, R/P60 (J.J.S.); National Institutes of Health Grant P42-ES07381; U.S. Environmental Protection Agency Grant R823890; the MIT/WHOI Joint Doctoral Program; and the NIEHS Division of Intramural Research.

* Corresponding author. Fax: 1-508-457-2169.

E-mail address: jstegeman@whoi.edu (J.J. Stegeman).

¹ Abbreviations used: AA, arachidonic acid; CYP, cytochrome P450; CYPOR, NADPH-cytochrome P450 reductase; DHET, *vic*-dihydroxyeicosatrienoic acid; EET, *cis*-epoxyeicosatrienoic acid; HETE, hydroxyeicosatetraenoic acid; PFB, pentafluorobenzyl; SRS, substrate recognition site; *Sf9*, *Spodoptera frugiperda* 9 cell line; TPA, 12-*O*-tetradecanoyl phorbol 13-acetate; SSPE, standard saline-phosphate-EDTA; PBS, phosphate-buffered saline; TMS, trimethylsilyl.

AA is catalyzed predominantly by CYP4 enzymes [8]. P450 metabolism of AA occurs in nonmammalian vertebrates [9,10]; however, except for studies with recombinant chick CYP1As and the recently described fish CYP2Ns [11] the identity of P450s catalyzing AA metabolism in nonmammalian vertebrate species is unknown. Knowledge of AA metabolism by P450s in early diverging vertebrates could help to elucidate the significance of those metabolites and the regulation of their formation in vertebrates in general. Conservation of CYP function in AA metabolism would suggest that a particular pathway is of phylogenetically broad biological importance, while lack of conservation would suggest evolutionary divergence in processes controlled by AA and, presumably, in AA catalysts.

Here we report on the cloning of three novel P450s from the teleost fish *Fundulus heteroclitus*. Sequence alignments indicate that these sequences constitute a new P450 subfamily, CYP2P. These new CYP2Ps are most similar to mammalian CYP2Js and to the recently discovered fish CYP2Ns, suggesting a hypothesis that there are conserved functions in these subfamilies. Thus, we addressed whether the novel fish CYP2Ps are related functionally to the CYP2Js, by accomplishing baculovirus expression and catalytic analysis of one of the new genes (CYP2P3). The results prompted a further analysis of selected AA metabolites formed by certain mammalian CYP2Js. We also compared aspects of the regulation of CYP2P3 and CYP2Js, related to possible physiological functions. The results establish that CYP2P3 is an early vertebrate arachidonic acid catalyst and reveal a striking similarity between CYP2P3 and certain of the CYP2Js with respect to regio- and enantioselective patterns of AA metabolism. Thus, sequence similarities, supported by similar catalytic function, tissue distribution, and regulation, indicate that the newly described fish CYP2P subfamily and the mammalian CYP2J subfamily are functionally as well as structurally related. Significantly, the CYP2Ns also have been shown to be AA epoxygenases. The CYP2J, CYP2N, and CYP2P subfamilies form a clade of related vertebrate CYP enzymes that are involved in AA metabolism and that probably have arisen from a common, ancestral gene.

Materials and methods

Materials. [^{14}C]Arachidonic acid was from DuPont–NEN. Triphenylphosphine, α -bromo-2,3,4,5,6-pentafluorotoluene, *N,N*-diisopropylethylamine, and diazald were from Aldrich, and RNA Stat-60 was from Tel Test B., Inc. Nick translation labeling kits were from Promega. Alkoxyresorufins were from Molecular Probes (Eugene, OR, USA). Other chemicals and reagents were from Sigma (St. Louis, MO, USA) unless

otherwise specified. *F. heteroclitus* were obtained from Scorton Creek (Sandwich, MA, USA), held in flow-through seawater, at 20 °C, at the Woods Hole Oceanographic Institution, and fed TetraMin fish diet (Tetra, Blacksburg, VA, USA).

Libraries and screening. The killifish genomic library was constructed in Lambda Fix II from a male fish (Stratagene). It had an amplified titer of 5×10^9 pfu/ml and insert sizes from 9 to 23 kb. A killifish λ gt10 liver cDNA library was obtained from Dr. D. Crawford (University of Missouri, Kansas City, MO, USA). A killifish liver cDNA library constructed in Uni-ZAP XR vector (Stratagene) (a gift from Dr. Sibel Karchner) also was screened.

Approximately 5×10^5 phage from the λ gt10 liver cDNA library were screened with two degenerate oligonucleotide probes end-labeled with [γ - ^{32}P]ATP (DuPont–NEN). Probes were designed essentially as previously described [11], based on alignments of CYP2 protein sequences representing CYP2 subfamilies from a variety of mammalian species (rat 2A1, 2B1, 2B2, 2G1, 2D1, and 2E1; mouse 2A5; human 2B1 and 2F1; rabbit 2B4, 2C3, and 2C4; dog 2C21) as well as chicken 2H1 and 2H2 and CYP101 from *Pseudomonas putida*. Conserved regions corresponding to α -helices in CYP101 [12] were chosen for oligonucleotide design, as they tend to be more conserved than substrate binding regions. Probes were designed corresponding to amino acid residues 144–160 and 349–355 of CYP2A1, respectively, 5'-CTGCAGCTCGAGGAGC GVATYCAGGASGARG C-3' and 5'-GGATCCTCTAGATSACBGCVTCNGT GTAKGGCA-3', with two restriction enzyme sites at the 5' ends. Fish codon usage tables [13] were used to reduce degeneracies.

Hybridizations were done in $6 \times$ SSPE, $0.05 \times$ Blotto, and 20% formamide at 42 °C overnight. In this screening approximately 90 positive clones were identified. Thirty-five of these were subcloned into pBluescript SK(+) and cycle sequenced by the dideoxy chain termination method using DNA polymerase (Epicentre Technologies) and infrared labeled primers (LI-COR). Approximately 6×10^5 phage from the Uni-ZAP XR liver cDNA library were screened with different sequence fragments isolated from the λ gt10 library. The fragments were random-primer labeled with [α - ^{32}P]dCTP using Rediprime (Amersham). Hybridizations were done in $6 \times$ SSPE, $0.05 \times$ Blotto, and 20–50% formamide at 42 °C overnight. Positive clones were isolated from each library, rescued into pBluescript SK(+), and sequenced in forward and reverse directions, using a Li-Cor Model 4000.

Approximately 5×10^5 phage from the Lambda FIX II library were plated with XL1-Blue *Escherichia coli* as host. Probes and hybridization conditions were identical to those used for the λ gt10 library. A 14-kb clone was restriction enzyme digested, subcloned in pBluescript

SK(+), sequenced as above, and determined to be a CYP2 (classified as CYP2P1). A cDNA for this CYP2 was amplified using 1 µg of total RNA from killifish liver and reverse transcribed with MuLV reverse transcriptase. The CYP2P1-specific oligonucleotide primers were used in a polymerase chain reaction with *Taq* polymerase (Perkin–Elmer Cetus) to amplify the CYP2P1 cDNA. The CYP2P1 primers spanned the entire CYP2P1 coding sequence and were 5'-GACATG GAGACAATCCTG-3' (nucleotide residues -3 to 15 of CYP2P1) and 5'-ACGAGATACGGCACAGAG-3' (nucleotide residues 1476–1494 of CYP2P1). CYP2P1 amplified cDNA was TA cloned into pGEM-T Easy (Promega) and sequenced as above.

The nucleotide sequences reported in this paper have been deposited with GenBank under Accession Nos. AF117341, AF117342, and AF117343.

Phylogenetic analysis. Phylogenetic analyses were conducted using both amino acid and nucleotide sequences for six killifish CYP2 genes and representatives of all other CYP2 subfamilies. All three nucleotide positions were used in the nucleotide analyses. Both maximum-parsimony and distance methods, using the minimum evolution criterion (neighbor-joining algorithm) [14] were used to construct the trees. Bootstrap analyses [15] were used to assess relative confidence in the topologies.

RNA analyses. RNA was prepared from killifish tissues using RNA Stat-60 according to the manufacturer's instructions. Total RNA (10 µg) was denatured and electrophoresed on 1.0% agarose gels containing 0.41 M formaldehyde and transferred to nylon membranes by downward alkaline capillary transfer as described [16]. The blots were hybridized with the CYP2P cDNAs labeled with [α -³²P]dCTP by nick-translation. Hybridizations were at 42 °C in 50% formamide, 6× SSPE, 1% (w/v) SDS, and 100 µg/ml heat-denatured calf-thymus DNA. Loading and transfer of RNA were monitored by detection of ethidium bromide stain in the gels and on the filters. Correlation between the stain on the filters and the amount of RNA was ascertained by probing the filters with labeled ribosomal RNA (data not shown). Gel images were recorded with a Kodak DCS digital camera and printed from Adobe PhotoShop, without modification.

Heterologous expression of recombinant CYP2P3. Heterologous expression of proteins encoded by the cDNA classified as CYP2P3 and human NADPH-cytochrome P450 oxidoreductase (CYPOR) cDNAs in *Sf9* insect cells was accomplished according to previously described methods [11,17,18]. Fish P450s readily accept electrons from mammalian CYPOR, supporting their catalytic function [19]. The CYP2P3 cDNA was subcloned into a pAcUW51-CYPOR shuttle vector [18] (kindly provided by Dr. Cosette Serabjit-Singh, Glaxo Wellcome), and protein was expressed using the Bacu-

loGold baculovirus expression system (Pharmingen, San Diego, CA, USA). Cultured *Sf9* insect cells were cotransfected with the transfer vector and linearized wild-type BaculoGold viral DNA in a CaCl₂ solution. Recombinant viruses were plaque purified and the presence of CYP2P3 cDNAs was confirmed by PCR analysis. *Sf9* cells, grown in spinner flasks at a density of 1.5–2.0 × 10⁶ cells/ml, were infected with a high-titer CYP2P3-CYPOR recombinant viral stock in the presence of 5 µM hemin or 5 µM δ -aminolevulinic acid hydrochloride [20]; cells were harvested 72 h after infection and washed twice with phosphate-buffered saline, and microsomal fractions were prepared [17]. P450 content was determined spectrally by the method of Omura and Sato [21] using a Shimadzu UV-3000 spectrophotometer. Microsomes were prepared also from *Sf9* insect cells coexpressing rat CYP2J3 and CYPOR [22]. Partially purified recombinant human CYP2J2 was obtained as before [17].

Arachidonic acid metabolism. *Sf9* cell microsomes with expressed CYP2P3 or CYP2J3 were resuspended to a final reaction volume in 0.05 M Tris–Cl buffer (pH 7.5) containing 0.15 M KCl, 0.01 M MgCl₂, 8 mM sodium isocitrate, and 0.5 units of isocitrate dehydrogenase/ml and equilibrated at 30 °C with constant mixing for 2 min before the addition of [1-¹⁴C]AA (25–55 µCi/µmol, 70–100 µM final concentration). Reactions were initiated by adding NADPH (1 mM final concentration) and continued at 30 °C with constant mixing. For reconstitution of CYP2J2, purified recombinant CYP2J2 was mixed with rat liver CYPOR (1 µM each, final concentration) in the presence of sonicated *L*- α -dilauryl-*sn*-glycerol 3-phosphate (50 µg/ml, final concentration). After 20 min at room temperature, the enzyme mixture was resuspended and equilibrated and AA metabolism reactions were initiated as above. At various times, reaction products were extracted into ethyl ether, dried under a nitrogen stream, resolved by reverse-phase HPLC, and quantified by online liquid scintillation using a Radiomatic Flo-One B detector (Radiomatic Instruments, Tampa, FL, USA) [23]. Uninfected *Sf9* cells, *Sf9* cells expressing only CYPOR, and reactions without NADPH were used as negative controls.

Individual EETs were identified by comparing their reverse-phase and normal phase HPLC properties with those of authentic standards and by GC/MS analysis [23–25]. For chiral analysis, the EETs were resolved by HPLC and collected batchwise, derivatized to the corresponding EET-pentafluorobenzyl (PFB) or EET-methyl esters, purified by normal-phase HPLC, resolved into the corresponding antipodes by chiral-phase HPLC, and quantified by liquid scintillation as described previously [26]. 19-HETE was identified based on coelution with authentic standard on reverse- and normal-phase HPLC and by GC/MS analysis [27,28]. Chiral analyses of 19-HETE was performed on naph-

thylated 19-HETE methyl esters using a Pirkle covalent D-phenyl glycine column (5 μ m, 4.6 \times 250 mm; Regis Chemical, Morton Grove, IL, USA) equilibrated with hexane 99.75%/isopropanol 0.25% at 1 ml/min [6]. Under these conditions, the retention times for 19(*R*)- and 19(*S*)-HETE are 76 and 80 min, respectively, with a resolution factor of 0.93.

Quantification of endogenous EETs and DHETs. EETs and DHETs in fish liver and intestine were quantified by methods similar to those used for eicosanoids in human heart and intestine [17,29]. Individual tissues frozen in liquid nitrogen were homogenized in 15 ml of PBS containing triphenylphosphine (5–10 mg). Homogenates were extracted twice under acidic conditions with two volumes of chloroform:methanol (2:1) and once more with an equal volume of chloroform. Organic phases were combined and evaporated in tubes containing [1-¹⁴C]8,9-EET, 11,12-EET, and 14,15-EET and [1-¹⁴C]8,9-DHET, 11,12-DHET, and 14,15-DHET as internal standards (55–57 μ Ci/ μ mol, 30–60 ng, each). Saponification to recover phospholipid-bound EETs and DHETs was followed by silica column purification. Eluent containing the radiolabeled internal standards and endogenous EETs/DHETs was resolved into individual regioisomers by HPLC as described [30]. Aliquots of individual EET-PFBs or DHET-PFB-trimethylsilyl (TMS) ethers were dissolved in dodecane and analyzed by GC/MS on a Kratos Concept ISQ mass spectrometer (Kratos Analytical, Ramsey, NJ, USA) operating under negative ion chemical ionization conditions, at 5.3 keV accelerating potential, at a mass resolution of 1200, and using methane as a bath gas. EETs were quantified by selected ion monitoring at *m/z* 319 (loss of PFB from endogenous EET-PFB) and *m/z* 321 (loss of PFB from [1-¹⁴C]EET-PFB standards). DHETs were quantified by selected ion monitoring at *m/z* 481 (loss of PFB from endogenous DHET-PFB-TMS) and *m/z* 483 (loss of PFB from [1-¹⁴C]DHET-PFB-TMS internal standards). The EET-PFB/[1-¹⁴C]EET-PFB and DHET-PFB/[1-¹⁴C]DHET-PFB ratios were calculated from the integrated values of the corresponding ion current intensities. The 5,6-isomers were not quantified due to their instability.

Metabolism of other substrates. Benzphetamine *N*-demethylation activity of recombinant CYP2P3 was assessed using the same microsomal preparations and reaction conditions used for AA metabolism, but with benzphetamine (2 mM final concentration) as the substrate. The reaction product (formaldehyde) was quantified according to the method of Nash [31]. Ethoxyresorufin, pentoxyresorufin, methoxyresorufin, and benzyloxyresorufin *O*-dealkylase activities of recombinant CYP2P3 and CYP2J3 were assessed by measuring the resorufin reaction products using a Cytofluor fluorescence plate reader (Millipore), as before [32]. In each case blank reactions were run with micro-

somes from uninfected *Sf9* cells, with microsomes from cells expressing CYP2P3 but not CYPOR, and/or reactions without NADPH.

Eicosanoid synthesis and modifications. The [1-¹⁴C]EET internal standards were synthesized from [1-¹⁴C]AA (55–57 μ Ci/ μ mol) by nonselective epoxidation as described [33]. Racemic and enantiomerically pure EETs were prepared by total chemical synthesis according to published procedures [34–37]. Methylations were performed using an ethereal solution of diazomethane [38]. PFB esters were formed by reaction with pentafluorobenzyl bromide as before [30]. Trimethylsilyl ethers were prepared using 25% (v/v) bis(trimethylsilyl)trifluoroacetamide in anhydrous pyridine [39]. Mid-chain HETE standards were purchased (Cayman Chemical). 19-HETE was synthesized as described [40].

Experimental treatments. All animal studies were conducted in accordance with principles and procedures outlined in the NIH Guide for the Care and Use of Laboratory Animals and approved by the WHOI or NIEHS Committees on Animal Care and Use.

Killifish. Just before the experiment, female fish that had been held in clean, flowing 20 °C water for more than 6 months were acclimated to 15 °C, a temperature at which they tolerate fasting well. Six fish were sacrificed at the start of the experiment and intestinal tissues were frozen immediately in liquid nitrogen for RNA analyses. Foregut, midgut, and hindgut were prepared separately. Twenty-four fish were fed excess TetraMin throughout the experiment; the rest were held without feeding. After 10 days of feeding or fasting, six fish from each group were sacrificed and tissues were frozen in liquid nitrogen. After 17 days, six fish in each group were given intraperitoneal injections of TPA in 80% normal saline/19.8% acetone/0.2% ethanol (vehicle) at 0.02 μ g TPA/g fish. Control fish were injected with vehicle alone or were uninjected. Six of the fasted fish were fed excess TetraMin. Fish were sacrificed 72 h later, and tissues were frozen in liquid nitrogen for RNA analyses. Equal amounts of tissue from the six fish were pooled prior to analysis. RNA from foregut was degraded and was not analyzed. The duration of fasting in these studies is consistent with the time of fasting used in studies of lipid and carbohydrate metabolism and gene regulation in fishes [41,42].

Rats. Adult male Fisher 344 rats were fed NIH 31 rodent chow (Agway, St. Mary, OH, USA) ad libitum, fasted 48 h, fasted 48 h and then refed for 6 h, or fasted 48 h and then refed for 24 h prior to sacrifice. All animals were allowed to drink water ad libitum and housed individually in suspended, metabolic cages to control coprophagy. All fasted animals had reduced body weight (–10%) and were ketotic as evidenced by increased plasma β -hydroxybutyrate and strongly positive urinary ketones. Animals were sacrificed by lethal CO₂ inhalation and exsanguinated by cardiac puncture.

Small intestines, livers, and kidneys were frozen in liquid nitrogen and used to prepare microsomal fractions by differential centrifugation as described [43].

Protein immunoblotting. Polyclonal anti-human CYP2J2 IgG, which cross-reacts with rat CYP2J3 and CYP2J4 but not with other known rat P450s [22], was raised in New Zealand White rabbits against the purified, recombinant CYP2J2 protein and affinity purified as described previously [17]. For immunoblotting, microsomal proteins were resolved by electrophoresis in SDS–10% (w/v) polyacrylamide gels (80 × 80 × 1 mm) (Novex, San Diego, CA, USA) and transferred electrophoretically to nitrocellulose membranes. Membranes were immunoblotted using the specific primary antibody, goat anti-rabbit IgG conjugated to horseradish peroxidase (Bio-Rad, Richmond, CA, USA), and the ECL Western Blotting Detection System (Amersham Life Sciences, Buckinghamshire, England) as described [22].

Results

Molecular cloning of the CYP2Ps. Screening of killifish genomic DNA and liver cDNA libraries with oligonucleotide probes to conserved regions in CYP2 genes resulted in identification of three new sequences that were related to the CYP2s. Initially, one sequence was isolated from the genomic library as one exon; sequence comparisons with known CYP2 genes resulted in classification of this killifish sequence into a new subfamily designated CYP2P, and the gene was designated CYP2P1. A full-length clone was later isolated from the genomic library and a full-length coding region cDNA obtained by RT-PCR from killifish liver RNA. Partial sequences for two related genes were isolated from the λ gt10 liver cDNA library and later retrieved as full-length clones from the Uni-ZAP liver cDNA library. Comparisons with known CYP2 genes resulted in these additional killifish sequences being classified into the new CYP2P subfamily, and they were designated CYP2P2 and CYP2P3 by the P450 Nomenclature Committee (<http://drnelson.utmem.edu/CytochromeP450.html>).

Including the 5' and 3' noncoding domains, the CYP2P2 cDNA is 2.1 kb, and the CYP2P3 cDNA is 1.9 kb. Open reading frames for CYP2P1, CYP2P2, and CYP2P3 are 1494 bp each, coding for proteins of 498 amino acids. The CYP2P nucleotide sequences share 79–84% identity with each other and 53–57% identity with the recently described CYP2Ns [11]. The deduced amino acid sequences of CYP2Ps share 71–79% identity with each other and 50–52% identity with the CYP2Ns. Alignment with representatives of other CYP2 subfamilies showed that CYP2P predicted protein sequences were most closely related to the mammalian CYP2Js,

with 46–50% shared identity. A sequence, PPGP, thought to be at the carboxyl end of the membrane anchor [44], was at positions 41–44 in all three CYP2P proteins. Each contained a putative heme binding peptide typical of CYP (Fig. 1); this peptide was F S A G K R V C L G in CYP2P1 and CYP2P3, and F S T G K R V C L G in CYP2P2, with a conserved cysteine that donates the thiolate fifth ligand to the heme iron at position 443 in each.

CYP2P1 gene structure and transcription elements. The total length of the CYP2P1 gene is ~11 kb and is separated into nine exons by eight intervening intron sequences. All of the splicing junctions (see Fig. 1) conform to the GT/AG rule [45]. The size of the CYP2P1 gene (~11 kb) is similar to that of rat CYP2B2 but not rat CYP2B1 (14 kb vs 23 kb) [46].

The 5' promoter region of CYP2P1 was analyzed for putative transcription elements using MatInspector [47], which identifies potential regulatory motifs by automatic searches with a library of precompiled nucleotide distribution matrices of regulatory consensus sequences. The CYP2P1 promoter region contains five putative barbiturate-responsive elements (Barbie boxes [48]), consistent with the structure of many mammalian CYP2 genes which possess Barbie boxes in their 5' promoter regions. Other putative regulatory sequences included multiple activator protein binding sites as well as sites for interferon regulatory factors, estrogen receptors, sterol regulatory element binding proteins 1, and NF- κ B.

Phylogenetic analyses of CYP2 genes. Two sets of phylogenetic analyses were done. The first used the majority of the coding sequences (>94%) to infer the phylogenetic relationships between selected members of known CYP2 gene subfamilies. The 5' and 3' untranslated regions were excluded due to length variations and resulting uncertain alignments. A total of 1422 nucleotide positions were compared, and 1267 sites (85%) were informative. A total of 472 amino acid positions were compared, and 411 sites (87%) were informative. The CYP2Ps were most closely related to the CYP2Js and the CYP2Ns. A second set of analyses used only the residues in the six regions thought to be involved in substrate recognition, as originally inferred for CYP2 genes by Gotoh [12]. Of the 228 nucleotides and 76 amino acids in the six putative SRSs, 205 nucleotide (90%) and 68 amino acid sites (89%) were informative. The topologies of the trees (e.g., Fig. 2) suggest that the SRSs of the CYP2Ps are related somewhat more closely to the mammalian CYP2Js than are the killifish CYP2Ns.

We compared the amino acid sequences for the putative SRSs among the three killifish CYP2Ps and between the CYP2Ps and the CYP2Js. The percentage identity for the sum of residues in the SRSs between any two of the CYP2Ps is 4–6% less than the percentage

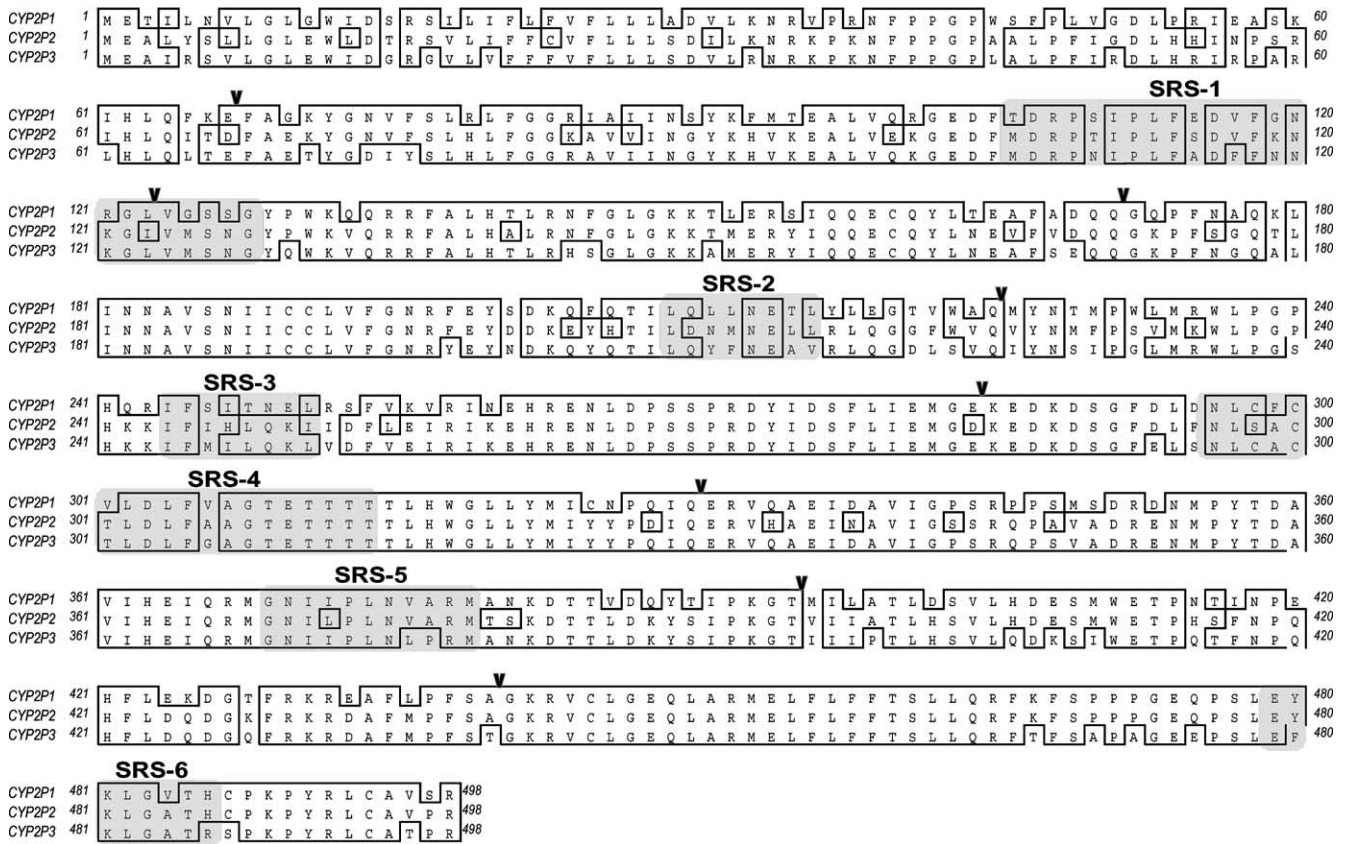


Fig. 1. Deduced amino acid sequences and alignment of killifish CYP2P1, CYP2P2, and CYP2P3. The shaded regions indicate the putative SRSs. Exon-intron boundaries are indicated by arrows.

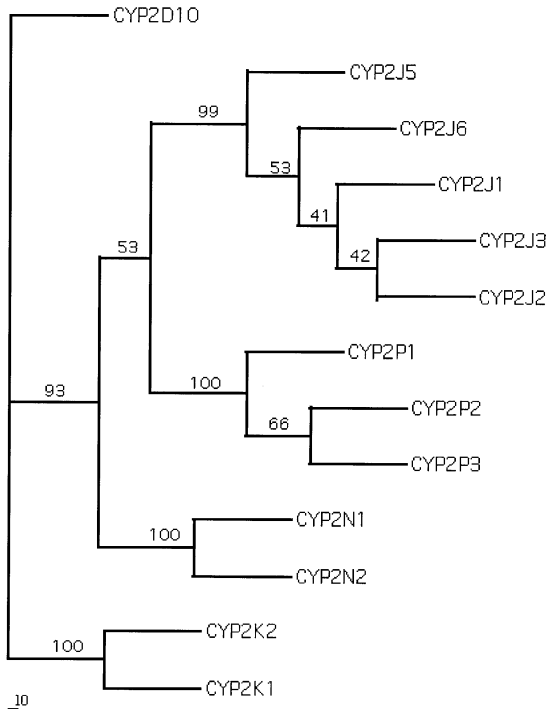


Fig. 2. Minimum evolution distance (Fitch-Margoliash) tree of sequences in the putative SRS regions. Bootstrap values shown represent 100 replicates and indicate the relative confidence in the topology.

identity in the full amino acid sequences between those same pairs; the average percentage identity among the SRSs was about 70% and among the full sequences was 74%. This is consistent with divergent substrate specificities among the CYP2Ps. The identity between the CYP2Ps and the CYP2Ns [11] was also less for the SRSs than the full-length sequences; average percentage identity among SRSs was 46% and among full-length sequences was 51%. In contrast, the opposite was found comparing the SRSs of either CYP2P1 or CYP2P3 and all of the CYP2Js examined. In those comparisons the percentage identities over the SRSs averaged 50%, somewhat higher than over the entire coding region (48%). This suggests a somewhat greater structural similarity in substrate recognition between some CYP2Ps and CYP2Js.

Tissue distribution. Probing RNA blots with the CYP2P cDNAs revealed that CYP2P1, CYP2P2, and CYP2P3 transcripts were expressed in intestine and liver; under high-stringency conditions of assay, expression was not seen in testis, ovary, kidney, gill, heart, brain, or muscle (not shown). The CYP2P1 probe hybridized most strongly with a 1.8-kb band in midgut but also hybridized with 5.5-, 3.6-, and 2.5-kb bands in liver (not shown). The CYP2P2 probe also hybridized with

four bands in these tissues (Fig. 3), the smallest of which was only 1.1 kb, suggesting that it might be a degradation product. The other bands were 2.8-, 2.3-, and 2.0-kb in size. The CYP2P3 probe hybridized strongly with a 2.5- and a 1.6-kb band and occasionally very faintly with a 2.3-kb band, in both liver and intestine (Fig. 3). Whether these multiple CYP2P-like transcripts are separate genes or alternatively spliced variants is not known. In liver, individual fish showed differences in expression levels of the two major bands, and there was no clear difference in expression between male and female fish (e.g., Fig. 3). In intestine, the expression was similar between individuals, but differed between different regions of the intestine (Fig. 3), with midgut generally showing higher expression than other regions.

Baculovirus expression and metabolism of arachidonic acid by CYP2P3. CYP2P3 was selected for expression studies, as it was the first full-length sequence obtained and showed a greater relative identity in SRS sequences to the CYP2Js, suggesting the hypothesis of functional

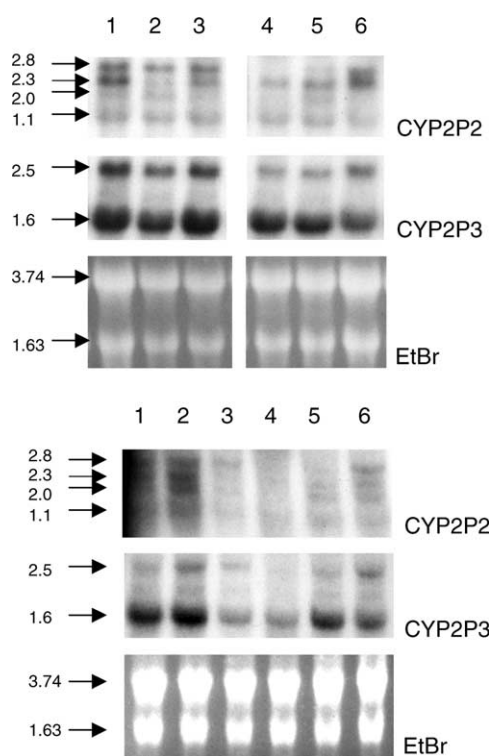


Fig. 3. Northern analyses of CYP2P3 mRNA in *F. heteroclitus* liver and intestine. In the first set total RNA preparations from livers of individual fish were probed with CYP2P cDNAs as described under Materials and methods. Lanes represent samples of liver from individual male (lanes 1–3) and female (lanes 4–6) fish. Arrows show sizes in kilobases. Ethidium bromide (EtBr) shows relative loading. In the second set, total RNA was obtained from sections of intestine from a single male (lanes 1–3) and a single female (lanes 4–6) fish. RNA from foregut (lanes 1 and 4), midgut (lanes 2 and 5), and hindgut (lanes 3 and 6) was probed with CYP2P cDNAs as indicated. Arrows show sizes in kilobases. EtBr shows relative loading.

similarities. Microsomes from *Sf9* cells expressing recombinant CYP2P3 showed typical P450 spectra with an absorbance peak near 450 nm when reduced and complexed with carbon monoxide. CYP2P3 was recovered in the low spin state, and the level of expression of recombinant CYP2P3 was between 3 and 10 nmol of spectral P450/liter of infected cells.

When incubated with AA in the presence of NADPH and an NADPH-regenerating system, microsomal fractions from cells expressing both recombinant CYP2P3 and recombinant CYPOR catalyzed AA metabolism at a rate of 0.135 nmol/nmol P450/min at 30 °C. The major products of AA oxidation were identified by comparing the reverse- and normal-phase HPLC properties of each product with the HPLC elution properties of authentic standards and by GC/MS analysis of the metabolites. No metabolites were formed in the absence of NADPH (Fig. 4; –NADPH), by microsomes from uninfected cells or by microsomes from cells expressing CYPOR but not P450 (not shown). As shown in Fig. 4, CYP2P3 formed 14,15-EET, 11,12-EET, and 8,9-EET as the major products; epoxidation at the 5,6-olefin was not detected. The three EETs were produced in roughly equal amounts and together accounted for 83% of the total metabolites (Table 1). CYP2P3 also formed a single HETE, 19-HETE, which made up the remaining 17% of total metabolites.

Stereochemical analysis of the EETs showed that expressed microsomal CYP2P3 preferentially formed the *R,S* enantiomer of 14,15-EET and the *S,R* enantiomer of the 8,9-EET; optical purities were 72 and 76%, respectively (Table 1). In contrast, the 11,12-EET was formed as a nearly racemic mixture (Table 1). Stereochemical analysis of 19-HETE formed by expressed CYP2P3 revealed a strong preference for 19(*R*)-HETE, with an optical purity of 78% (Table 1).

To fully compare the metabolites formed by CYP2P3 to those formed by the CYP2Js, it was necessary to examine further the products formed by the CYP2Js. Reverse-phase HPLC chromatograms of lipid-soluble products formed during incubations of AA with recombinant CYP2J2 and CYP2J3 also are shown in Fig. 4. The regioselectivity of CYP2J2 is similar to that of CYP2P3. The identification of 19-HETE formation by CYP2J2 (Fig. 4) is a new finding; in previous studies CYP2J2 was found to produce this same chromatographic peak but at the time that peak was examined only for 5,6-DHET [17]. CYP2J3 also forms the same EETs as CYP2P3, but with somewhat different proportions. As determined previously, CYP2J3 also forms large amounts of 19-HETE, but chiral analysis was not performed [22]. We therefore performed a chiral analysis of the 19-HETE formed by recombinant CYP2J3, which revealed a preference for 19(*R*)-HETE, with an optical purity of 70%, quite similar to CYP2P3 (Table 2).

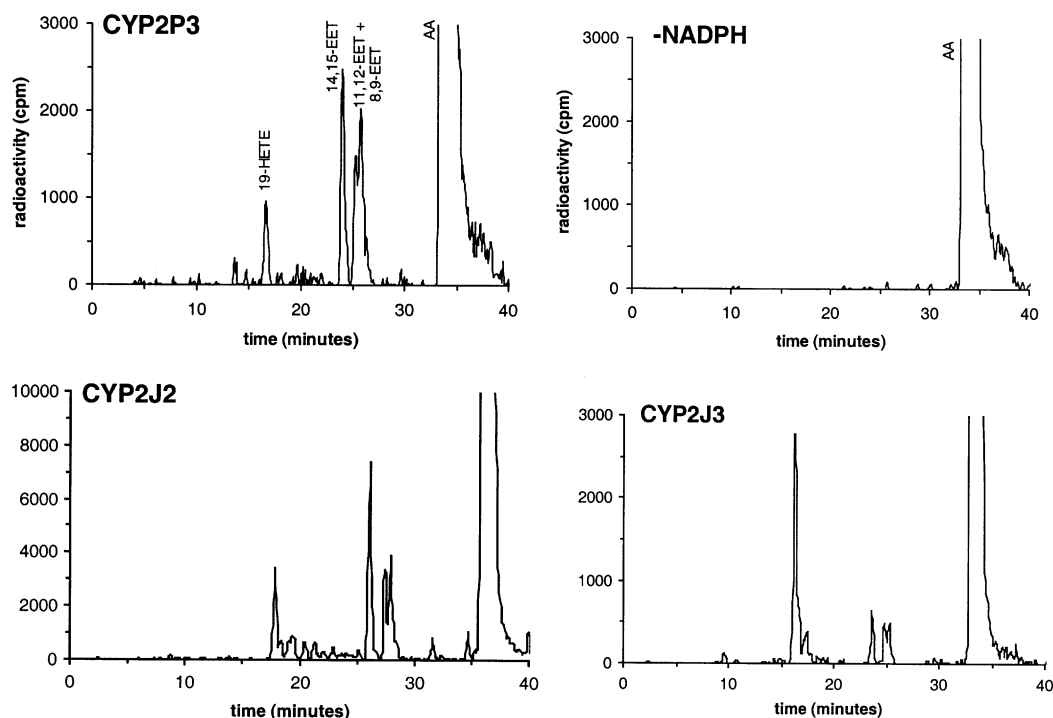


Fig. 4. reverse-phase HPLC chromatograms of the organic soluble metabolites formed by incubation of arachidonic acid with recombinant P450s. Microsomal fractions prepared from CYP2P3/CYPOR-transfected *S9* insect cells or from CYP2J3/CYPOR-transfected *S9* insect cells or purified, recombinant CYP2J2 plus CYPOR (bottom) were incubated at 30 °C with [1-¹⁴C]arachidonic acid (70–100 μM, final concentration) with NADPH (1 mM, final concentration) and an NADPH-regenerating system. “–NADPH” shows results of incubation of CYP2P3/CYPOR insect cell microsomes in the absence of NADPH. After 1 h, the reaction products were extracted and resolved by HPLC; peaks for the CYP2Js were as described [17,22]. Peak identifications were made by comparing the HPLC properties of individual peaks with those of authentic standards using both reverse-phase and normal-phase HPLC and GC/MS. For CYP2J2, the peak with retention time 17–18 min was previously identified as containing 5,6-DHET [16]; however, further analysis revealed that it contains 19-HETE as the major component and 5,6-DHET only as a minor component. Ordinate, radioactivity in cpm; abscissa, time in minutes.

Table 1

Regiochemical and stereochemical composition of EETs and 19-HETE produced by recombinant CYP2P3

Product	Distribution (% of total)	Enantioselectivity	
14,15-EET	30	72 (%R, S)	28 (%S, R)
11,12-EET	27	48 (%R, S)	52 (%S, R)
8,9-EET	26	24 (%R, S)	76 (%S, R)
5,6-EET	Not detected	—	—
19-HETE	17	78 %R	22 %S

The activity of recombinant CYP2P3 in *S9* microsomes was assayed in the presence of NADPH and an NADPH-regenerating system as described under Materials and methods. After 1 h, the EET products were extracted into ethyl ether, resolved into individual regioisomers by reverse-phase HPLC, derived to corresponding EET-PFB or EET-methyl esters, purified by normal-phase HPLC, and resolved into the corresponding antipodes by chiral-phase HPLC. 19-HETE was resolved into antipodes as described under Materials and methods. Values shown are averages of at least three different experiments. Individual results of those experiments differed from the mean by <5%.

Benzphetamine and alkoxyresorufins. CYP2P3 metabolized benzphetamine at a substantial rate (catalytic turnover: 3.3 nmol/nmol P450/min). In contrast, alkoxyresorufin *O*-dealkylase activities catalyzed by CYP2P3 were very slow, 0.002 nmol/nmol P450/min with methoxyresorufin or ethoxyresorufin and <0.001 nmol/nmol P450/min with pentoxyresorufin or benzyloxyresorufin as substrates. Expressed CYP2J2 and CYP2J3, analyzed here, had similarly slow rates of activity (about 0.001 nmol/nmol P450/min) with the alkoxyresorufin substrates.

EETs and DHETs in fish tissues. Analysis of lipid fractions from killifish liver and intestine revealed that both organs contained approximately 200 ng EETs/g tissue (Fig. 5). 14,15-EET was the predominant isomer recovered from both tissues, comprising 52 and 47% of the total EETs in liver and intestine, respectively. The 11,12-EET and 8,9-EET were recovered in lower and similar amounts from these tissues. Fish liver and intestine also contained approximately 75 ng total DHET/g tissue (Fig. 5), suggesting that EETs are hydrated by epoxide hydrolase *in vivo*. The 8,9-, 11,12-, and 14,15-

Table 2

Regio- and stereochemistry of the major arachidonic acid metabolites produced by killifish CYP2P3, human CYP2J2, and rat CYP2J3

CYP	Regiochemistry (% of total) EETs				
	14,15-	11,12-	8,9-	5,6-	19-HETE
2P3	30	27	26	<1	17
2J2	37	18	24	1	20
2J3	13	9	9	1	68

CYP	Enantioselectivity (% enantiomer)							
	14,15-EET		11,12-EET		8,9-EET		19-HETE	
	(R,S)	(S,R)	(R,S)	(S,R)	(R,S)	(S,R)	(R)	(S)
2P3	72	28	48	52	24	76	78	22
2J2	76	24	49	51	47	53	—	—
2J3	43	57	62	38	60	40	70	30

Some of the data for AA metabolites formed by CYP2J2 and CYP2J3 are from previous studies [17,22]. The 19-HETE data are new findings in this study. Dashes indicate not examined.

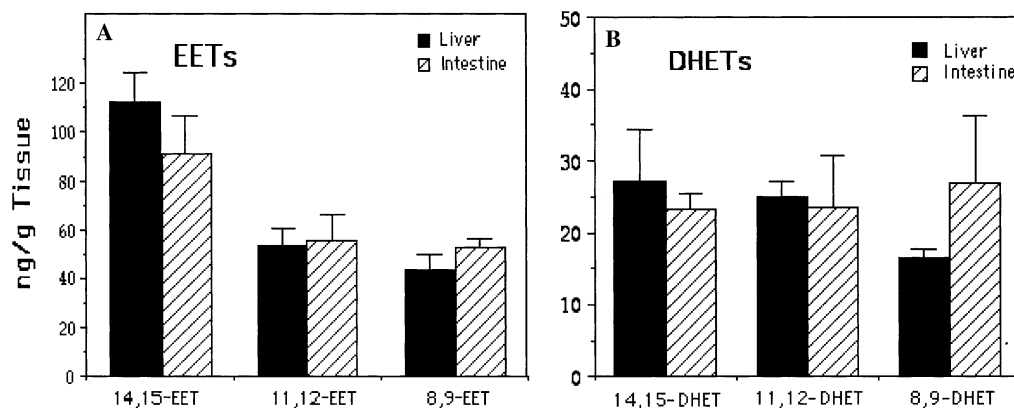


Fig. 5. Endogenous EETs and DHETs in killifish liver and intestinal tissues. Levels of the EET (A) and DHET (B) regioisomers were quantified by HPLC and GC/MS as described under Materials and methods. Values shown are means of three individual experiments \pm standard errors.

DHET were recovered in nearly equal amounts from liver and intestine (Fig. 5). Intestine also contained about 40 ng 5,6-DHET/g tissue; 5,6-DHET was not detected in liver (data not shown).

Regulation of CYP2P3 and CYP2J by fasting and phorbol ester. The relatively high levels of EETs and the abundance of CYP2P transcripts in killifish intestine suggest that CYP2Ps might have a role in intestine. To investigate possible factors regulating CYP2P expression in vivo, we examined the levels of CYP2P transcripts in intestine of fed fish and fasted fish. The effect of the phorbol ester TPA on CYP2P3 expression also was examined, in both fed fish and fasted fish. TPA treatment was selected as phorbol esters can affect free AA concentrations [49] and might therefore influence expression or activity of AA-metabolizing enzymes. TPA treatment depressed the transcript levels of CYP2P2 and CYP2P3 in midgut of fed fish (Fig. 6). Prolonged fasting itself slightly depressed the levels of the 2.5-kb transcript of CYP2P3 in midgut and more strongly in hindgut (Fig. 6). CYP2P2 transcript expres-

sion showed a stronger response to fasting than did CYP2P3. CYP2P1 on the other hand showed little response to TPA treatment or fasting either in midgut or in hindgut. However, unlike the other two genes, fasting and then refeeding for 3 days resulted in an increased expression of CYP2P1, but such a refeeding effect was muted or not evident with CYP2P2 or CYP2P3.

Effects of fasting on CYP2J protein expression in rats. The results above indicate that the CYP2P3 is phylogenetically related to the mammalian CYP2Js and show that members of these two gene subfamilies share similar enzymological properties in the metabolism of AA to EETs and HETEs. To investigate whether members of the CYP2P and CYP2J subfamilies are regulated by similar factors, we then examined the levels of CYP2J proteins in various tissues of rats following fasting and during refeeding. The levels of rat intestinal CYP2J3/4 protein were significantly reduced following 48 h of fasting (Fig. 7). In contrast, hepatic and renal expression of CYP2J3/4 remained unchanged by fasting and re-

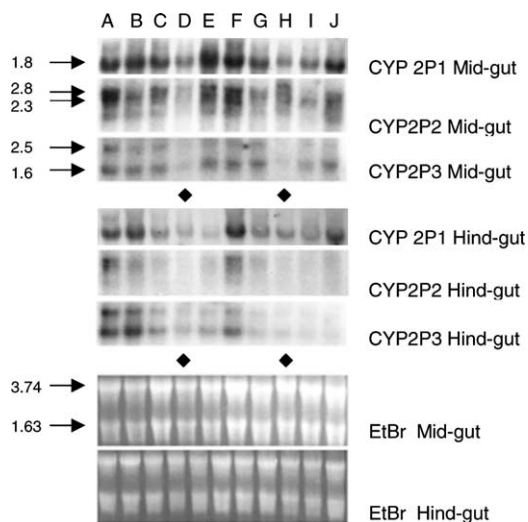


Fig. 6. Northern analyses of CYP2P gene expression in intestinal tissues of fed fish, fasted fish, and TPA-treated fish. Lanes A–E are fed fish; lanes F–J are fasted fish. Treatment groups are as follows: (A) time zero, (B) fed for 10 days, (C) fed for 20 days, (D) fed for 20 days and treated with TPA 3 days before sampling, (E) fed for 20 days and treated with vehicle 3 days before sampling, (F) fasted 10 days, (G) fasted 20 days, (H) fasted 20 days and treated with TPA 3 days before sampling, (I) fasted 20 days and treated with vehicle 3 days before sampling, (J) fasted for 20 days and refed for 3 days. The sizes of transcripts recognized by the CYP2P cDNAs are indicated on the left side. EtBr refers to ethidium bromide staining, showing relative loading between lanes. Diamonds indicate the lanes with TPA-treated fish.

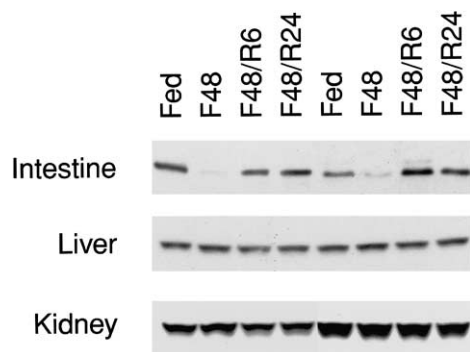


Fig. 7. Effect of fasting on CYP2J3/4 expression in intestine, liver, and kidney of rat. Tissue microsomal fractions were prepared from rats that were either fed, fasted for 48 h (F48), fasted 48 h and refed 6 h (F48/R6), or fasted 48 h and refed 24 h (F48/R24). Twenty micrograms of protein was applied to each lane, electrophoresed, transferred to nitrocellulose, and immunoblotted with anti-human CYP2J2 IgG as described under Materials and methods. The antibody used cross-reacts with rat CYP2J3 and CYP2J4, but not with other known rat P450s.

feeding (Fig. 7). Thus, the effects of fasting on intestinal CYP2J expression in rats were similar to the effects of fasting on intestinal CYP2P2 and 2P3 expression in killifish, suggesting that these phylogenetically related P450 genes are regulated in a similar fashion.

Discussion

The CYP2 gene family includes a bewildering array of genes in more than 25 gene subfamilies and CYP2s metabolize an extraordinary number of both exogenous and endogenous substrates. However, physiological or endogenous functions are still obscure even for most of the mammalian CYP2s. Analysis of CYP2 genes in nonmammalian vertebrates may provide insights into the functional relationships and possibly the basis for diversification among the CYP2s. A search for homologues with catalytic properties conserved among CYP2s from taxonomically distant groups, e.g., fish and mammals, could be particularly revealing. In this study we have cloned three new CYP genes, defining a new P450 subfamily, the CYP2Ps, and coexpressed one of these, CYP2P3, with CYPOR in a baculovirus system to evaluate functions of this new P450. Analysis of arachidonic acid metabolism by microsomes from insect cells expressing recombinant CYP2P3 showed that this CYP formed only three EETs and 19-HETE, a highly regioselective metabolism of AA.

The mammalian CYPs most similar in sequence to the CYP2Ps are the CYP2Js. The similarities in sequence and tissue distribution between the CYP2Ps and the CYP2Js led us to hypothesize that members of these different subfamilies would have similar catalytic functions.

In order to address the functional similarity between the CYP2P and the CYP2J enzymes, we also examined further the AA metabolites formed by CYP2J2 and CYP2J3 and especially the chirality of selected products of these mammalian CYPs. Analysis of the regioisomeric and enantiomeric selectivity of the eicosanoid product formation revealed remarkable similarities between the catalytic properties of killifish CYP2P3, human CYP2J2, and rat CYP2J3 (Table 2). The similarities between CYP2P3 and CYP2J2 are particularly striking. These CYP form similar amounts of the 14,15-, 11,12-, and 8,9-EETs. Moreover, these enzymes show nearly identical chiral specificity for formation of the 14,15- and 11,12-EETs, favoring epoxidation at the *re, si* face of the 14,15-olefin and forming racemic 11,12-EET (Table 2). All three enzymes synthesize 19-HETE as the only HETE, and CYP2P3 and CYP2J3 form 19-HETE with remarkably similar specificities for the *R* enantiomer. (CYP2J2 enantioselectivity for 19-HETE formation is not known.) The highly similar regio- and enantioselectivities lead us to conclude that these fish and mammalian CYPs have very similar active site topologies, effecting a similar orientation of AA in the active center of these enzymes.

Killifish CYP2P3 and several CYP2Js also have similar specificities with xenobiotic substrates. Thus, CYP2P3, CYP2J1 [50], and CYP2J3 all metabolize benzphetamine at similar rates (3.3, 3.9, and 3.0 nmol/

nmol CYP/min, respectively). CYP2P3 and CYP2J3 both dealkylate ethoxy-, methoxy-, pentoxy-, or benzyloxyresorufin at rates barely exceeding the limit of detection. These properties of CYP2P3 and selected CYP2Js indicate further that some enzymes in these subfamilies from taxonomically distant species are catalytically as well as structurally similar.

The catalytic similarity of these enzymes is particularly noteworthy since catalytic functions of microsomal P450s can be strongly affected by minor structural differences [51]. The degree of amino acid identity in putative SRSs between CYP2P3 (or CYP2P1) and selected CYP2Js was somewhat greater than the identity found comparing full-length sequences of the proteins. The greater rather than lesser identity in the putative SRS sequences is consistent with the thought based on catalytic function that CYP2P3 and selected CYP2Js have similar active site structures. Identifying critical active site residues will be important to better understand these similarities.

Phylogenetic analysis clusters another recently described teleost CYP2 subfamily, the CYP2Ns, with the CYP2Js and CYP2Ps. The CYP2Ns also metabolize AA [11]. Thus, these three subfamilies (CYP2J/CYP2N/CYP2P) form a clade of genes coding for enzymes involved in AA metabolism. However, the CYP2Ns oxidize AA with regio- and enantioselectivities quite distinct from those of CYP2P3. Both CYP2N1 and CYP2N2 form 8,9-EET as the dominant EET, with a strong preference ($\geq 90\%$) for the *R,S* enantiomer, and both CYP2Ns catalyze hydroxylation of AA to numerous HETEs but form little or no 19-HETE [11].

Endogenous AA metabolites. EETs and their corresponding hydration products the DHETs were detected as endogenous constituents of killifish liver and intestinal tissues, indicating that AA epoxidation and EET hydration occur *in vivo* in these fish. The content of EETs in the liver of the killifish was three- to fourfold greater than recently reported for liver of the marine fish scup [10], but less than the levels of EETs commonly detected in mammalian liver. In contrast, killifish intestine had a fivefold greater content of EETs than has been reported for human intestine [29], suggesting that AA epoxygenase(s) may be more active in killifish intestine than in mammalian intestine. Endogenous EETs in killifish liver and intestine included 14,15-, 11,12-, and 8,9-EETs, products that could result from epoxidation of endogenous AA pools in killifish tissues by several CYPs, including CYP2P3 and the CYP2Ns, which also are expressed in killifish liver and gut, although the relative contribution of the CYP2P3 enzyme to formation of these products *in vivo* is unclear. The presence of 5,6-EET in intestine also implies the action of a P450 catalyst distinct from CYP2P3 and the CYP2Ns, none of which oxidized the 5,6-olefin *in vitro*.

CYP2P regulation. Fasting decreased the transcript levels of CYP2P3 and CYP2P2 genes in the lower intestine, while TPA strongly decreased the abundance of CYP2P3 transcripts in midintestinal tissues of both fasted and fed fish. TPA mimics diacylglycerol [52], causing a decrease in protein kinase C (PKC) activity, also shown to result from fasting [53]. Protein kinase C influences multiple intracellular pathways [53] and as a result can modulate many different cellular processes. Thus, TPA and fasting effects on CYP2P transcript levels both might occur through an involvement of PKC, although further studies are needed to elucidate the mechanisms underlying the inhibitory effects of TPA and fasting on CYP2P expression. Notably, the examination of intestinal CYP2J3 expression in rats, reported herein, showed that this enzyme also is suppressed by fasting. This similarity between the CYP2Ps and the CYP2Js suggests further that members of these CYP subfamilies could function similarly in intestinal physiology.

The EETs have potent vasodilatory effects in the rat intestinal microcirculation [54], and 19-HETE has been shown to be vasoactive [55]. The high levels of CYP2P3 transcript in liver and intestine, the documentation that EETs are endogenous constituents of these tissues, and the regulation of CYP2Ps by fasting suggest that these eicosanoids have biological functions in fish, and possibly a regulatory role in intestinal processes. Eicosapentaenoic acid (EPA) and docosahexaenoic acid (DHA), fatty acids which are more abundant than AA in marine fish, also yield metabolites that are biologically active. It will be interesting to determine whether EPA or DHA are specifically oxidized by CYP2Ps, which could suggest similar involvement by the CYP2Js and may support physiological roles for EPA and DHA metabolites. The CYP2Ps also may oxidize retinoids, suggested by the finding that CYP2Js catalyze oxidation of retinoids [56].

In summary, we have identified three new P450s defining a new vertebrate CYP2 subfamily, the fish CYP2Ps. In a large multigene family such as the CYP2s, concerted evolution can obscure orthologous relationships between genes [57], which otherwise might be derived from molecular phylogenetic analysis. The CYP2Ps, the CYP2Ns and the mammalian CYP2Js form a distinct clade within the CYP2 gene family and appear to have arisen from a common ancestral gene. Diversity in this clade is increasing as additional members are being identified in various species genomes. The sequence identities, similar tissue distribution, and similar enzyme properties among selected CYP2Ps and CYP2Js are particularly striking. These similarities together indicate that these two subfamilies bear a relationship to one another not evident from their separate classification. Analysis of the full complement of CYP2Ps and CYP2Js in taxonomically distant species

should reveal the extent of conservation of functions within these CYP subfamilies, which may in turn point to endogenous roles conserved in this increasingly complex clade of CYP2 genes.

Acknowledgments

We thank Dr. Cosette Serabjit-Singh, for providing the pAcUW5-CYPOR vector, and Dr. John Falck for providing synthetic EET and HETE standards. We also thank Jennifer Schlezinger, Eli Hestermann, Joyce Goldstein, Richard Philpot, Mark Hahn, and John Curtis for helpful comments during the work and on the manuscript. This is Contribution No. 9702 of the Woods Hole Oceanographic Institution.

References

- [1] B. Escalante, D. Erlj, J.R. Falck, J.C. McGiff, *Science* 251 (1991) 799–802.
- [2] M.G. Wade, G. Van Der Kraak, *Gen. Comp. Endocrinol.* 90 (1993) 109–118.
- [3] G.C. Liggins, R.J. Fairclough, S.A. Grieves, *Recent Prog. Horm. Res.* 29 (1973) 111–149.
- [4] A. Sellmayer, W.M. Uedelhoven, P.C. Weber, J.V. Bonventre, *J. Biol. Chem.* 266 (1991) 3800–3807.
- [5] W.L. Smith, *Biochem. J.* 259 (1989) 315–324.
- [6] E.H. Oliw, *Prog. Lipid Res.* 33 (1994) 329–354.
- [7] J.C. McGiff, *Annu. Rev. Pharmacol. Toxicol.* 31 (1991) 339–369.
- [8] J.H. Capdevila, D.C. Zeldin, A. Karara, J.R. Falck, in: *Advances in Molecular and Cell Biology*, JAI Press Inc, 1996, pp. 317–339.
- [9] D. Gilday, M. Gannon, K. Yutzey, D. Bader, A.B. Rifkind, *J. Biol. Chem.* 271 (1996) 33054–33059.
- [10] J.J. Schlezinger, C. Parker, D.L. Zeldin, J.J. Stegeman, *Arch. Biochem. Biophys.* 353 (1998) 265–275.
- [11] M.F. Oleksiak, S. Wu, C. Parker, S.I. Karchner, J.J. Stegeman, D.C. Zeldin, *J. Biol. Chem.* 275 (2000) 2312–2321.
- [12] O. Gotoh, *J. Biol. Chem.* 267 (1992) 83–90.
- [13] L.M. Fitzgerald, A. Rodrigues, G. Smutzer, *Mol. Mar. Biol. Biotech.* 2 (1993) 112–119.
- [14] N. Saitou, M. Nei, *Mol. Biol. Evol.* 4 (1987) 406–425.
- [15] J. Felsenstein, *Evolution* 39 (1985) 783–791.
- [16] P. Chomczynski, *Anal. Biochem.* 201 (1992) 134–139.
- [17] S. Wu, C.R. Moomaw, K.B. Tomer, J.R. Falck, D.C. Zeldin, *J. Biol. Chem.* 271 (1996) 3460–3468.
- [18] C.A. Lee, S.H. Kadwell, T.A. Kost, C.J. Serabjit-Singh, *Arch. Biochem. Biophys.* 319 (1995) 157–167.
- [19] A.V. Klotz, J.J. Stegeman, B.R. Woodin, E.A. Snowberger, P.E. Thomas, C. Walsh, *Arch. Biochem. Biophys.* 249 (1986) 326–338.
- [20] F.J. Gonzalez, S. Kimura, S. Tamura, H.V. Gelboin, *Methods Enzymol.* 206 (1991) 93–99.
- [21] T. Omura, R. Sato, *J. Biol. Chem.* 239 (1964) 2370–2378.
- [22] S. Wu, C. Weina, E. Murphy, S. Gabel, K.B. Tomer, J. Foley, C. Steenbergen, J.R. Falck, C.R. Moomaw, D.C. Zeldin, *J. Biol. Chem.* 272 (1997) 12551–12559.
- [23] J.H. Capdevila, J.R. Falck, E. Dishman, A. Karara, *Methods Enzymol.* 187 (1990) 385–394.
- [24] J.H. Capdevila, P. Yadagiri, S. Manna, J.R. Falck, *Biochem. Biophys. Res. Commun.* 141 (1986) 1007–1011.
- [25] R.A. Clare, S. Huang, M.V. Doig, G.G. Gibson, *J. Chromatogr.* 562 (1991) 237–247.
- [26] T.D. Hammonds, I.A. Blair, J.R. Falck, J.H. Capdevila, *Anal. Biochem.* 182 (1989) 300–303.
- [27] J. Capdevila, L.J. Marnett, N. Chacos, R.A. Prough, R.W. Estabrook, *Proc. Natl. Acad. Sci. USA* 79 (1982) 767–770.
- [28] J.R. Falck, S. Lumin, I. Blair, E. Dishman, M.V. Martin, D.J. Waxman, F.P. Guengerich, J.H. Capdevila, *J. Biol. Chem.* 265 (1990) 10244–10249.
- [29] D. Zeldin, J. Foley, S. Goldsworthy, M. Cook, J. Boyle, J. Ma, C. Moomaw, K. Tomer, C. Steenbergen, S. Wu, *Mol. Pharmacol.* 51 (1997) 931–943.
- [30] A. Karara, E. Dishman, I. Blair, J.R. Falck, J.H. Capdevila, *J. Biol. Chem.* 264 (1989) 19822–19827.
- [31] T. Nash, *Biochem. J.* 55 (1953) 416–421.
- [32] J.J. Stegeman, M.E. Hahn, R. Weisbrod, B.R. Woodin, J.S. Joy, S. Najibi, R.A. Cohen, *Mol. Pharmacol.* 47 (1995) 296–306.
- [33] J.R. Falck, P. Yadagiri, J.H. Capdevila, *Methods Enzymol.* 187 (1990) 357–364.
- [34] E.J. Corey, A. Marfat, J.R. Falck, J.O. Albright, *J. Am. Chem. Soc.* 102 (1980) 1433–1435.
- [35] J.R. Falck, S. Manna, *Tetrahedron Lett.* 23 (1982) 1755–1756.
- [36] C.A. Moustakis, J. Viala, J.H. Capdevila, J.R. Falck, *J. Am. Chem. Soc.* 107 (1986) 5283–5285.
- [37] P. Mosset, D. Yadagiri, S. Lumin, J.H. Capdevila, J.R. Falck, *Tetrahedron Lett.* 27 (1986) 6035–6038.
- [38] J.H. Capdevila, B. Pranamik, J.L. Napoli, S. Manna, J.R. Falck, *Arch. Biochem. Biophys.* 231 (1986) 511–517.
- [39] N.A. Porter, J. Logan, V. Konotoyianidou, *J. Org. Chem.* 44 (1979) 3177–3181.
- [40] S. Manna, J.R. Falck, N. Chacos, J.H. Capdevila, *Tetrahedron Lett.* 27 (1983) 6035–6038.
- [41] I. Navarro, J. Gutierrez, J. Planas, *Comp. Biochem. Physiol. A* 102 (1992) 401–407.
- [42] G. Mourente, D.R. Tocher, *Biochim. Biophys. Acta* 1212 (1994) 109–118.
- [43] D.C. Zeldin, J.D. Plitman, J. Kobayashi, R.F. Miller, J.R. Snapper, J.R. Falck, J.L. Szarek, R.M. Philpot, J.H. Capdevila, *J. Clin. Invest.* 95 (1995) 2150–2160.
- [44] S. Yamazaki, K. Sato, K. Suhara, M. Sakaguchi, K. Mihara, T. Omura, *J. Biochem.* 114 (1993) 652–657.
- [45] R. Breathnach, P. Chambon, *Annu. Rev. Biochem.* 50 (1981) 349–383.
- [46] Y. Suwa, Y. Mizukami, K. Sogawa, Y. Fujii-Kuriyama, *J. Biol. Chem.* 260 (1985) 7980–7984.
- [47] K. Quandt, K. Frech, H. Karas, E. Wingender, T. Werner, *Nucleic Acids Res.* 23 (1995) 4878–4884.
- [48] A.J. Fulco, J.S. He, Q.W. Liang, in: *Cytochrome P450, 1994*, pp. 37–42.
- [49] S.M. Fischer, T.J. Slaga (Eds.), *Arachidonic Acid Metabolism and Tumor Promotion*, Martinus Nijhoff, Boston, 1985.
- [50] Y. Kikuta, K. Sogawa, M. Haniu, M. Kinosaki, E. Kusunose, Y. Nojimas, S. Yamamoto, K. Ichihara, M. Kusunose, Y. Fujii-Kuriyama, *J. Biol. Chem.* 266 (1991) 17821–17825.
- [51] R.L.P. Lindberg, M. Negishi, *Nature* 339 (1989) 632–634.
- [52] A.S. Kraft, W.B. Anderson, *Nature* 301 (1983) 621–623.
- [53] A.C. Newton, *J. Biol. Chem.* 270 (1995) 28495–28498.
- [54] D.R. Harder, W.B. Campbell, R.J. Roman, *J. Vasc. Res.* 32 (1995) 79–92.
- [55] M.A. Carroll, P.M. Garcia, J.R. Falck, J.C. McGiff, *J. Pharmacol. Exp. Ther.* 260 (1992) 104–109.
- [56] Q.-Y. Zhang, G. Raner, X. Ding, D. Dunba, M.J. Coon, L.S. Kaminsky, *Arch. Biochem. Biophys.* 353 (1998) 257–264.
- [57] L. Hood, J.H. Campbell, S.C.R. Elgin, *Annu. Rev. Genet.* 9 (1975) 305–353.